

The redox interaction of nano cobalt sulphate (NCS) and fuchsin acid (FA) at different temperatures was investigated using a new glassy carbon electrode with multicarbon nanotube filled nano composite.

Mohamed Fathi*¹, Esam A. Gomaa², Abdel Hamid.Farouk¹, Shereen E. Salem², Hamada M.Killa¹

¹) Chemistry Department, Faculty of Science, Zagazig University, Egypt.

²) Chemistry Department, Faculty of Science, Mansoura University, Egypt.

Corresponding author: mohamed.fathi257@yahoo.com

ABSTRACT: Ball milling was employed to prepare nano compounds of tantalum pentoxide and cobalt sulphate that used a Retsch MM2000 apparatus and three stainless steel balls with diameters of 12 mm. The new filled nano composite working electrode was created by combining nano tantalum pentoxide to multicarbon nanotubes and carbon in a specific ratio, and the final nano paste was applied to the tip of a glassy carbon electrode. Cyclic voltammetry was used to examine the redox reaction of NCS alone and in combination with FA in 0.1M KBr at two different temperatures (292.15&297.15) K. At the two temperatures used, various solvation and kinetic parameters were evaluated and discussed. In addition, in order to study complexation, various thermodynamic data, including stability constants, complexation Gibbs free energies, enthalpies, and entropies, were measured for the communication of NCS to FA. Their values were then discussed.

KEYWORDS: Cyclic voltammetry, Thermodynamic parameters, 5C5S, Molecular docking, Nano cobalt sulphate salt, Fuchsin acid, stuffed nano glassy carbon electrode.

Date of Submission: 18-09-2022

Date of acceptance: 06-11-2022

I. INTRODUCTION

One of the most often used electrochemical techniques for obtaining qualitative data on an electrolytic method is cyclic voltammetry. It is accomplished through assessing the current as just a consequence of the applied voltage. It is possible. The current is calculated as just a result of the given potential, starting with the initial potential (E_i) and varying linearly up to the end value (E_f). When the potential reaches its final value, the potential scan's direction is reversed, and the scan occurred in the opposite direction in the same potential range. A three-electrode setup is used to perform this approach. While a potential is applied to the working electrode in relation to a reference electrode, an auxiliary (or counter) electrode is used to finish the electrical circuit by transferring electricity from the signal source to the other electrodes in solution. The number of electrons involved in the oxidation or reduction reaction, the formal potential, a system's stoichiometry, heterogeneous rate constants, and the diffusion coefficient of electroactive species can all be determined using cyclic voltammetry. Considering that cyclic voltammetry is an easy, quick, and sensitive method, it's often used to determine compounds like transition metals and antibiotics like fuchsin acid (FA). Cobalt compounds have gotten a lot of interest in recent years since they plays a big role in a lot of biochemical processes and are employed in a lot of different industries including industrial and medicinal chemistry [1-9]. Magnetic nanoparticles have made progress in research owing to their properties and prospective applications [10]. Magnetic nanoparticles such as cobalt sulphate have been shown to have potential uses in the areas of information storage, catalytic magnetics, medical diagnosis, and electrical characteristics. [11-13].

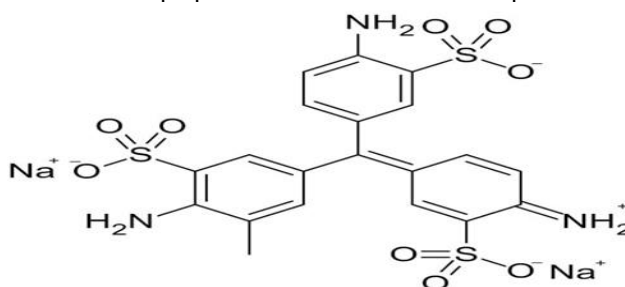
Because of its catalytic, electrical, and therapeutic applications, cobalt sulphate has got a lot of interest in recent years. It possesses three metastable phases with diverse crystallographic shapes, making it one of the most ferromagnetic materials. [14,15]. Cobalt salt is a chemical that is employed in the electrolytic and metal

plating industry sectors. [10]. It is used in protective coating to increase the deposited materials' smoothness, illumination, rigidity, and ductility. Rechargeable cells, pigments, and coatings for lithographic all employ it as a drier. It's also been used to raise hematocrit, haemoglobin, and erythrocyte levels in human patients with refractory anaemia, such as sickle-cell disease, thalassemia, and chronic kidney disease [15]. Antibiotics, often known as antibacterial, are antimicrobial drugs that are used to treat and prevent bacterial infections. Bacteria may be killed or inhibited by these substances. Antiprotozoal action is seen in a small number of antibiotics [16]. Acid fuchsin is a combination of homologues of basic fuchsin that have had sulfonic groups added to them. Jakub Natanson initially made fuchsin from aniline and 1,2-Dichloroethane in 1856. It can also be used to detect bacteria that are proliferating [17]. The study of metal complexes is a popular topic of research. Complex formation has got a lot of attention. Spectrophotometry, cyclic voltammetry, NMR spectrometry, calorimetry, potentiometry, and conductometry are some of the physicochemical techniques that can be employed to examine these complexation reactions. Basic thermodynamic research like enthalpy, entropy, and Gibbs free energy can be also determined [18-20]. Charge and size of the metal ion, type of metal ion, counter ion, nature of the ligand, temperature, and physical properties of solvents are all factors that affect complex stability. The value of the association constant can be calculated using the conductometric approach. The temperature dependence of the association constant can be used to compute the enthalpy change (ΔH) and entropy change (ΔS) of complexation reactions in various binary mixtures. This study is useful to understand the effect of ionic size, solvent composition, temperature and the nature of the complexing agent. Additionally, electrochemistry offers an effective methodologies for understanding the complexation reactions. For example, cyclic voltammetry techniques can be utilized to investigate the redox attitude of metal salts in the lack and existence of ligand and from which can be determined the stability constant of complex formed and thermodynamic parameters such as Gibbs free energy, The enthalpy change (ΔH) and entropy change (ΔS) for a system can be determined. This research is useful in understanding the effects of solvent composition, ionic size, temperature, and the complexing agent's nature. Electrochemistry also provides useful approaches for comprehending complexation reactions. For example, cyclic voltammetry technics may be utilized to explore the redox attitude of metal salts in the absence and presence of ligand, allowing the stability constant of the complex produced and thermodynamic characteristics like Gibbs free energy to be measured. A system's enthalpy change (ΔH) and entropy change (ΔS) can be calculated.

II. MATERIALS AND METHODS

Solvents and Materials

Perfect cobalt sulphate salt (CoSO_4) from Merck Corporation, fuchsin acid (FA) from Oxford Research lab, perfect potassium bromide salt (KBr) from Adwic Corporation, and bidistilled water with a conductivity of $2.9 \mu\text{S cm}^{-1}$ were utilized in this research. In addition, pure tantalum pento-oxide salt (Ta_2O_5) from BDH Middle East FZ LLC, graphite powder from Adwic Egypt, and carbon nano-tube from Egyptian Petroleum Research Institute were utilized in the prep work of the filled nano composite electrode.



Fuchsin acid (FA)
(Acid Violet 19)

Basic formula $\text{C}_{20}\text{H}_{17}\text{N}_3\text{Na}_2\text{O}_9\text{S}_3$
Molecular weight $585.53 \text{ g}\cdot\text{mol}^{-1}$

Nano salt preparation.

That used a ball-mill device of the Retsch MM2000 swing mill, granular cobalt sulphate salt (CoSO_4) was stirred for two hours to create nano cobalt sulphate (NCS). Ball milling was carried out at 20225 Hz and at 20 C with stainless steel tubes of volume 10 cm³ and three stainless steel balls of diameter (11×10^{-3}) m. In addition, nano tantalum pentoxide salt was synthesized from bulk tantalum pentoxide salt utilizing the same

ball milling method (Ta2O5). At last a transmission electron microscope (TEM) was employed to examine the nanoscale.

Preparation of glassy carbon electrodes with doped nano composites

To create a homogeneous paste, [81% graphite powder, 9% paraffin wax, 4% nano tantalum pentoxide, and 6% multi layers carbon nano tube] was thoroughly mixed. The resulting composite was then placed inside the electrode's tip (depth: 6×10^{-3} m). A copper wire was forced down the electrode to make an external electrical contact. The electrode's surface was touched up with a piece of weighting paper before being thoroughly washing the electrode with room temperature distilled water. The nano carbon composite that resulted was examined using a transmission electron microscope (TEM).

Analysis of cyclic voltammetry (CV)

The cyclic voltammetric studies were performed with a DY2000 multichannel potentiometer shipped from the United States. It was linked to a cell with three electrodes: a reference electrode of silver/silver chloride in saturated KBr solution, a working electrode of doped nano composite glassy carbon (DGC), and an auxiliary electrode of platinum wire. The surface of the doped nano composite glassy carbon electrode (DGC) was polished to a mirror finish using 1-0,03 micro alumina powder before being washed with absolute alcohol and doubly-distilled water to remove any adhering alumina particles. The electrode's area was (5.72×10^{-2}) cm². The system was utilized with a potential window of (0.4 to -1.5)V and variable scan rates (0.1, 0.05, 0.02, 0.01)V/sec at two distinct temperatures (292.15 and 297.15)K. Before each experiment, purification N₂ was passed through to ensure an inert atmosphere and diffusion experiment. The information was finally examined using the original software.

III. RESULTS AND DISCUSSION

Electron microscopy in transmission (TEM)

Nano tantalum pentoxide, multi-nano composite carbon composite of the utilized glassy carbon electrode, and nano cobalt sulphate salt were examined using a transmission electron microscope to determine their internal structure and size, as shown in Figure 1. Nano tantalum pentoxide salt was discovered to be in the deformed hexagonal shapes' designs, ranging from 18 nm to 23 nm in size, while nano cobalt sulphate was found to be in the shape of irregular spheres, measuring 62–69 nm in size.

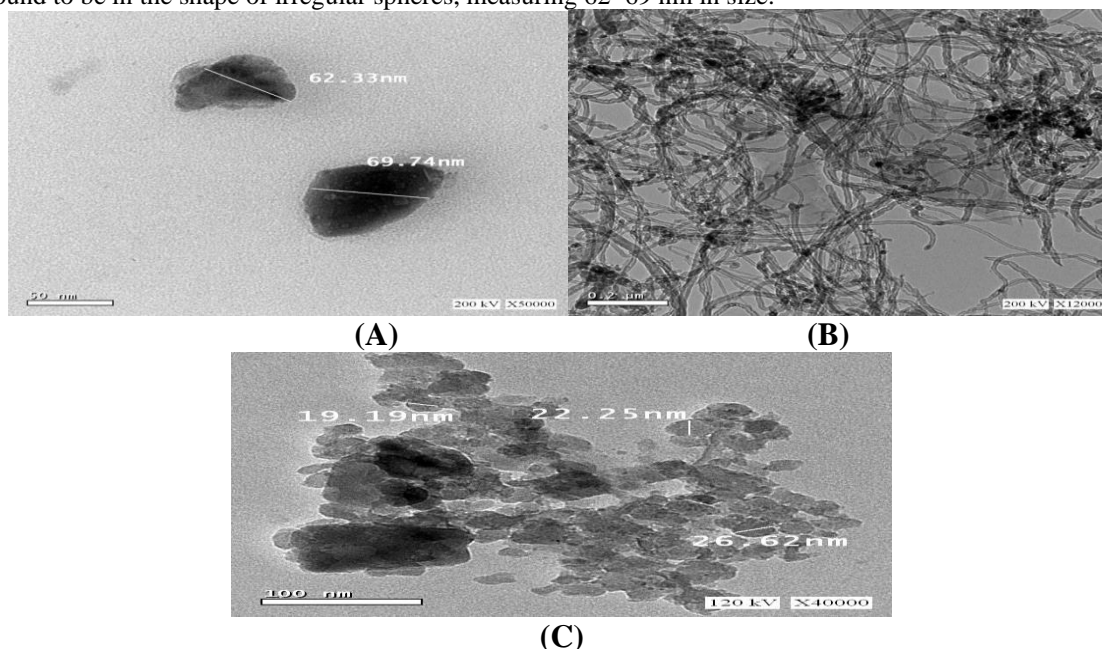


Fig.(1): TEM photos of (a) nano tantalum pentoxide salt (b) multi nano composite carbon dough of the utilised glassy carbon electrode (c) nano cobalt sulphate salt

Cyclic voltammetry (CV)

At two different temperatures, the electrochemical behaviour of nanocobalt sulphate salt (NCS) alone.

Effect of various NCS concentrations at 292.15 and 297.15K alone.

Using a DY2000 multichannel potentiometer at 292.15 and 297.15K, a filled nano glassy carbon electrode (DGC) was used to measure the cycles voltammogram of KBr (0.1) M, a supportive electrolyte, from (0.4 to -1.4)V. (Fig. 2). Then, by gradually addition of nano-Co²⁺ ions solution from 1 ml (1.77 x 10⁻³ M) to 6 ml (9.17 x 10⁻³ M) at 292.15 and 297.15K, the redox behaviour of nano-Co²⁺ was studied in 0.1 M KBr (Fig. 3). In the used window from 0.4 V to -1.5 V at the two utilized temperatures, one reduction wave was seen. The oxidation happened in two waves, as depicted in Fig. 3. The same pattern was also observed at both temperatures, with the higher temperature showing waves that were more clearly defined.

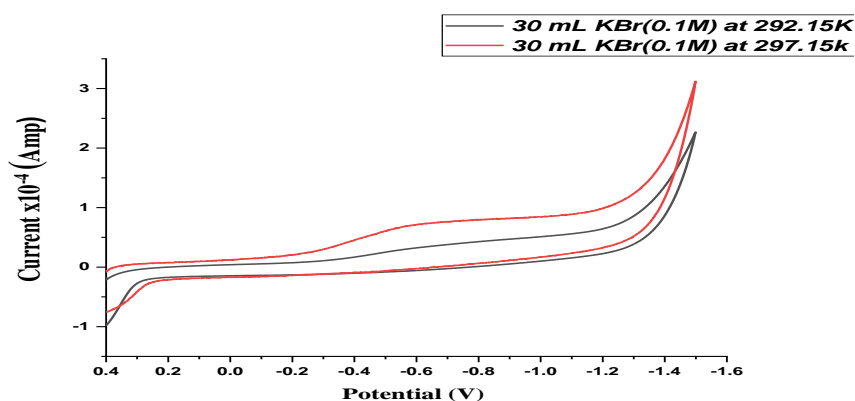


Fig.2: A 30 ml KBr (0.1) M cyclic voltammogram with 0.1 (V.sec⁻¹) scan rates at 292.15 and 297.15K

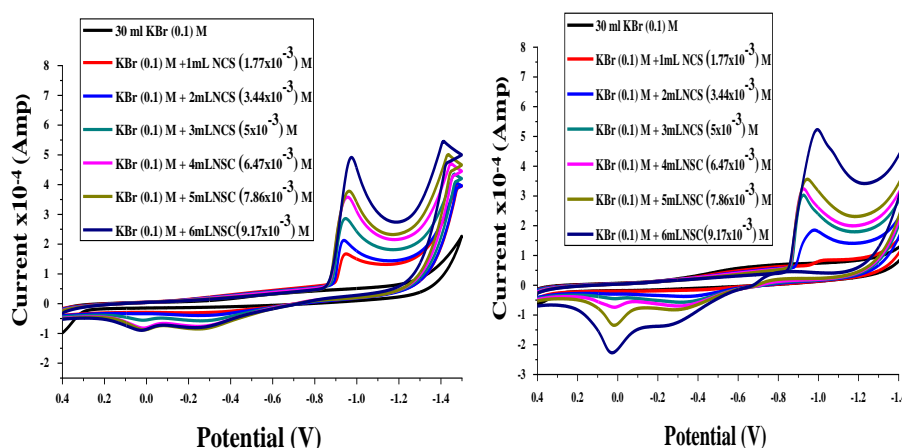


Fig.3: Impact of various NCS ratios at (a) 292.15K (b) 297.15K and scan speed 0.1 (V.sec⁻¹).

In order to study the electrochemical redox actions of nano Co²⁺ ions in KBr (0.1) M at steady state current, the following equations were applied to obtain and discuss cyclic waves [21-37].

$$i_p = 0.4463 n F A C (n F D v / R T)^{1/2} \quad \text{Randles Sevcik formula (1)}$$

$$\Delta E_p = E_{pa} - E_{pc} \quad (2)$$

$$k_s = 2.18 * [D_C \alpha_n F v / RT]^{1/2} * \exp [\alpha^2 n F \Delta E_p / RT] \quad (3)$$

$$\alpha_n = 1.857 RT / (E_p - E_{pc}/2) F \quad (4)$$

$$\Gamma = i_p 4RT / n^2 F^2 A v \quad (5)$$

$$(Q = n F A \Gamma) \quad (6)$$

in which i_p is the current in Amperes, A was the working electrode's surface area in centimetres squared, D was the diffusion coefficient in centimetres squared per second, v was the scan rate in volts per second, and C was the concentration of Co^{2+} , k_s was the standard heterogeneous electron transfer rate constant in cm/sec, α is the charge transfer coefficient, n_a was the number of electron transfers in the rate-determining step, $E_{pc/2}$ was the half-wave potential for the cathodic peak, and θ was the surface coverage in $\text{mol}\cdot\text{cm}^{-2}$. The surface coverage can be calculated using the amount of charge used during the reduction or adsorption of the adsorbed layer Q . The calculated solvation and kinetic parameters are E_{p_a} (anodic peak potential), E_{p_c} (cathodic peak potential), I_{p_a} (anodic peak current), I_{p_c} (cathodic peak current), ΔE_p (peak potential difference), D_a (anodic diffusion coefficient), D_c (cathodic diffusion coefficient), k_s (electron transfer rate constant), Γ_a (anodic surface coverage), Γ_c (cathodic surface coverage), Q_a (anodic quantity of electricity) and Q_c (cathodic quantity of electricity) were tabulated in **Table.1 (a&b)**. It was observed from **Table.1 (a&b)** that E_p , I_p and D increased at higher temperature 297.15K than 292.15K. k_s had higher values at $(9.17 \times 10^{-4})\text{M}$ of FA at 297.15K. Q and Γ dropped at higher temperature 297.15K than 292.15K as result of the products' migration away from the electrode's surface due to of the temperature raise.

Table.1(a): The solvation and kinetic values of various NCS ratios at 292.15 K and scan speed 0.1 ($\text{V}\cdot\text{sec}^{-1}$).

| [M] x 10^{-3} | $E_{p,a}$ | $E_{p,c}$ | ΔE_p | ΔE_p (mV) | $(-I_{p,a}) \times 10^{-5}$ | $I_{p,c} \times 10^{-4}$ | $D_a \times 10^{-13}$ | $D_c \times 10^{-11}$ | k_s | $\Gamma_a \times 10^{-9}$ | $\Gamma_c \times 10^{-8}$ | $(-) Q_a \times 10^{-5}$ | $(+) Q_c \times 10^{-4}$ |
|-----------------|-----------|-----------|--------------|-------------------|-----------------------------|--------------------------|-----------------------|-----------------------|-------|---------------------------|---------------------------|--------------------------|--------------------------|
| 1.771 | 0.3195 | 0.9461 | 0.6266 | 626.61 | 1.62 | 1.17 | 4.403 | 2.315 | 6.553 | 0.739 | 0.535 | 0.8157 | 0.591 |
| 3.438 | 0.3195 | 0.9390 | 0.6195 | 619.48 | 2.59 | 1.63 | 2.989 | 1.191 | 4.101 | 1.180 | 0.744 | 1.302 | 0.821 |
| 5.000 | 0.2740 | 0.9490 | 0.6750 | 675.00 | 4.49 | 2.36 | 4.256 | 1.179 | 10.17 | 2.048 | 1.078 | 2.260 | 1.189 |
| 6.471 | 0.2721 | 0.9555 | 0.6834 | 683.36 | 6.28 | 3.08 | 4.973 | 1.200 | 10.99 | 2.865 | 1.407 | 3.162 | 1.553 |
| 7.857 | 0.2721 | 0.9651 | 0.6930 | 692.98 | 6.67 | 3.28 | 3.801 | 0.918 | 10.64 | 3.041 | 1.495 | 3.356 | 1.650 |
| 9.167 | 0.2740 | 0.9746 | 0.7006 | 700.59 | 7.15 | 4.42 | 3.212 | 1.225E-11 | 15.38 | 3.261 | 2.014 | 3.600 | 2.223 |

Table.1(b): Various NCS concentrations' solvation and kinetic characteristics at 297.15 K and 0.1 V/sec scan speed.

| [M] x 10^{-3} | $E_{p,a}$ | $E_{p,c}$ | ΔE_p | $(-I_{p,a}) \times 10^{-5}$ | $I_{p,c} \times 10^{-4}$ | $D_a \times 10^{-13}$ | $D_c \times 10^{-12}$ | k_s | $\Gamma_c \times 10^{-8}$ | $(+) Q_c \times 10^{-4}$ | $\Gamma_a \times 10^{-9}$ | $(-) Q_a \times 10^{-5}$ |
|-----------------|-----------|-----------|--------------|-----------------------------|--------------------------|-----------------------|-----------------------|--------|---------------------------|--------------------------|---------------------------|--------------------------|
| 1.77 | 0.4198 | 1.0242 | 0.6043 | 0.5033 | 0.2612 | 0.4249 | 1.144 | 0.583 | 0.121 | 0.133 | 0.2335 | 0.2577 |
| 3.44 | 0.3413 | 0.9760 | 0.6346 | 2.780 | 1.373 | 3.452 | 8.428 | 2.587 | 0.637 | 0.7033 | 1.290 | 1.423 |
| 5.00 | 0.3149 | 0.9254 | 0.6105 | 4.713 | 2.541 | 4.691 | 1.363 | 2.650 | 1.179 | 1.301 | 2.187 | 2.413 |
| 6.47 | 0.3043 | 0.9289 | 0.6245 | 5.903 | 2.749 | 4.393 | 9.527 | 2.679 | 1.275 | 1.408 | 2.738 | 3.023 |
| 7.86 | 0.2779 | 0.9462 | 0.6683 | 7.241 | 3.072 | 4.484 | 8.071 | 4.958 | 1.425 | 1.573 | 3.359 | 3.708 |
| 9.17 | 0.2169 | 0.9936 | 0.7766 | 12.73 | 4.746 | 10.18 | 14.15 | 46.493 | 2.202 | 2.430 | 5.907 | 6.520 |

Impact of various scan rates

At two distinct temperatures (292.15 and 297.15)K, the cyclic voltammogram of NCS (9.17×10^{-3} M) in KBr (0.1 M) was investigated at various scan speeds (0.1, 0.05, 0.02, and 0.01) ($V \cdot sec^{-1}$) Maxima were seen in Fig. 4. It is observed that by decreasing scan rates, both anodic and cathodic currents decreased but other solvation parameters like Γ_c , Γ_a , Q_c and Q_a are increased. The relation (i_p vs $v^{1/2}$) indicates the linear dependence of the peak current on the square root of the scan rate and the reaction is governed by diffusion controlled process. As a result of the adsorbed species' adsorption, catalysis, and electrocatalysis on the nano electrode surface. The volumetric behaviour was also explained by the conflict between adsorption and dehydration. Calculations of the solvation and kinetic values at various scan speeds were shown in Table 2. (a&b). The catalytic mechanism and minimum coverage were required to Γ_a and Γ_c . It was observed that the solvation and kinetic values increased by increasing temperature due to more solvation.

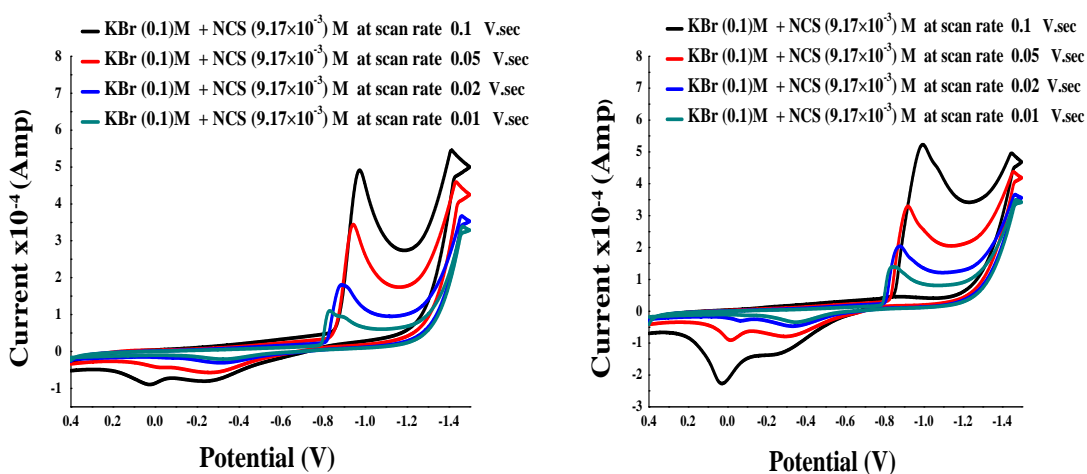


Fig.(4): Impact of various scan speeds of (9.17×10^{-3}) M NCS at (a) 292.15 K (b) 297.15 K.

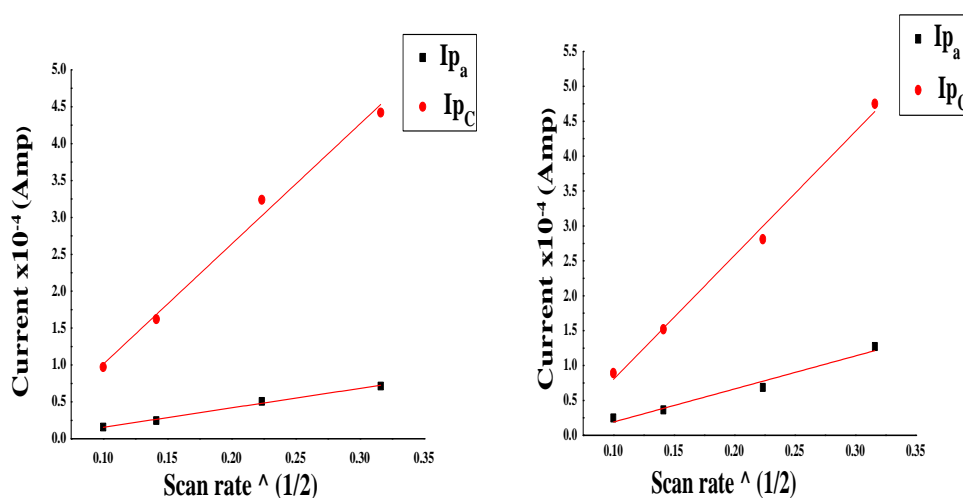
Table.2 (a): The solvation and kinetic values of (9.17×10^{-3})M NCS at various scan speeds and 292.15 K.

| v | E_{pa} | E_{pc} | ΔE_p | $(-I)_{pa}$ $\times 10^{-5}$ | I_{pc} $\times 10^{-4}$ | D_a $\times 10^{-13}$ | D_c $\times 10^{-12}$ | k_s | Γ_a $\times 10^{-9}$ | Γ_c $\times 10^{-8}$ | $(-)Q_a$ $\times 10^{-5}$ | $(+)Q_c$ $\times 10^{-4}$ |
|------|----------|----------|--------------|---------------------------------|------------------------------|----------------------------|----------------------------|-------|--------------------------------|--------------------------------|------------------------------|------------------------------|
| 0.10 | 0.2714 | 0.9756 | 0.7106 | 7.150 | 4.425 | 3.222 | 12.26 | 15.37 | 3.271 | 2.024 | 3.602 | 2.233 |
| 0.05 | 0.2718 | 0.9463 | 0.6572 | 5.070 | 3.251 | 3.228 | 13.21 | 6.272 | 4.626 | 2.966 | 5.092 | 3.273 |
| 0.02 | 0.3112 | 0.8871 | 0.5836 | 2.475 | 1.627 | 1.920 | 8.224 | 0.526 | 5.633 | 3.678 | 6.202 | 4.081 |
| 0.01 | 0.3214 | 0.8331 | 0.5181 | 1.596 | 0.980 | 1.591 | 5.928 | 0.122 | 7.245 | 4.437 | 7.983 | 4.896 |

Table.2 (b): The solvation and kinetic values of (9.17×10^{-3})M NCS at various scan speeds and 297.15 K.

| v | E_{pa} | E_{pc} | ΔE_p | $(-I)_{pa}$ $\times 10^{-5}$ | I_{pc} $\times 10^{-4}$ | D_a $\times 10^{-13}$ | D_c $\times 10^{-12}$ | k_s | Γ_a $\times 10^{-9}$ | Γ_c $\times 10^{-8}$ | $(-)Q_a$ $\times 10^{-5}$ | $(+)Q_c$ $\times 10^{-4}$ |
|------|----------|----------|--------------|---------------------------------|------------------------------|----------------------------|----------------------------|--------|--------------------------------|--------------------------------|------------------------------|------------------------------|
| 0.1 | 0.2169 | 0.9936 | 0.7766 | 12.73 | 4.746 | 10.18 | 14.15 | 46.493 | 5.907 | 2.202 | 6.520 | 2.430 |
| 0.05 | 0.2933 | 0.9453 | 0.6520 | 6.838 | 2.808 | 5.876 | 9.907 | 2.511 | 6.345 | 2.605 | 7.003 | 2.876 |
| 0.02 | 0.3332 | 0.8861 | 0.5529 | 3.646 | 1.523 | 4.177 | 7.289 | 0.234 | 8.458 | 3.533 | 9.336 | 3.900 |
| 0.01 | 0.3502 | 0.8321 | 0.4819 | 2.468 | 0.892 | 3.829 | 5.005 | 0.051 | 11.45 | 4.141 | 12.64 | 4.570 |

The Randless Sevicek equation [38–42] was utilized to relate the cathodic and anodic peak currents among with the square root of scan speed, and it yields straight lines to represent the diffusion process in **Figure**



5.

Fig.(5): Peak current and voltage relationship I_p (I_{pC} – I_{pA}) among the square root of various scan speeds at (a) 292.15K (b) 297.15K.

Electrochemical performance of nanocobalt sulphate solution (NCS) in existence of Fuchsin acid (FA) at two various temperatures.

Impact of various FA at 292.15 and 297.15K.

The electrochemical performance for the synthesized complex among NCS and FA was studied in 0.1M KBr and scan speed 0.1 (V.sec⁻¹) at 292.15 and 297.15K, **Fig.6**. It was observed that the maxima for Co²⁺ ions increased by adding Fuchsin acid (FA) in the reduction window due to the raise in the dehydration and catalysis of the adsorbed ions. This demonstrated that FA boosted the amount of adsorbed ions and ionisation in the aqueous solutions that were employed. **Table 3(a,b)** shows the solvation and kinetic characteristics of the reaction between NCS (9.17x 10⁻³)M and various FA concentrations at 292.15 and 297.15K and scan rate 0.1 V/sec. It was observed that the solvation values for nano cobalt sulfate decreased With the addition of Fuchsin acid (FA) and by increasing temperature 297.15 K due to complexation. Also the surface coverage values for Co²⁺ ions dropped With the addition of FA facilitating happened of linear cathodic maxima.

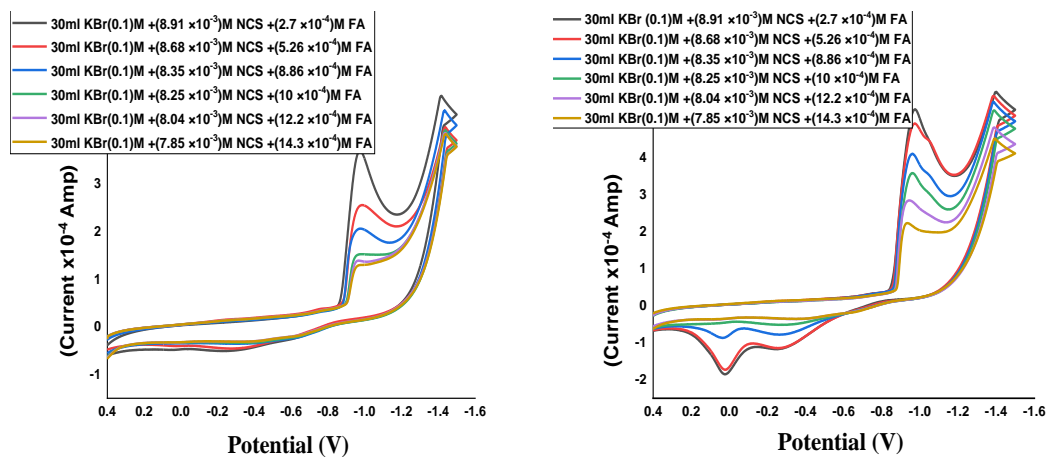


Fig.(6): Impact of various concentrations of FA at (a) 292.15K (b) 297.15K and scan speed 0.1 V/sec.

Table.3(a): Impact of various ratios of FA for the 292.15K redox region.

| conc of[M] x10 ⁻³ | conc of [L] x10 ⁻⁴ | Ep,a | Ep,c | ΔEp | (-)Ip,a x10 ⁻⁵ | Ip,c x10 ⁻⁴ | Da x10 ⁻¹⁴ | Dc x10 ⁻¹³ | Ks | (-) Q a x10 ⁻⁵ | (+) Qc x10 ⁻⁴ | Γ a x10 ⁻⁹ | Γ c x10 ⁻⁹ |
|------------------------------|-------------------------------|------------|------------|--------|---------------------------|------------------------|-----------------------|-----------------------|------------|---------------------------|--------------------------|-----------------------|-----------------------|
| 8.929 | 2.71 | 0.264 2 | 0.986 3 | 0.7222 | 4.79 | 2.88 | 15.21 | 55.22 | 14.09 9 | 2.41 0 | 1.452 | 2.184 | 13.1 6 |
| 8.684 | 5.26 | 0.284 5 | 0.982 6 | 0.6981 | 4.00 | 2.15 | 11.19 | 32.44 | 6.731 | 2.01 3 | 1.084 | 1.823 | 9.81 |
| 8.354 | 8.86 | 0.353 9 | 0.956 6 | 0.6028 | 3.36 | 1.51 | 8.555 | 17.16 | 0.880 | 1.69 3 | 0.758 | 1.534 | 6.86 9 |
| 8.250 | 10.0 | 0.368 3 | 0.954 2 | 0.5859 | 3.14 | 1.10 | 7.667 | 9.431 | 0.543 | 1.58 3 | 0.555 | 1.434 | 5.03 0 |
| 8.049 | 12.2 | 0.372 3 | 0.956 0 | 0.5836 | 2.99 | 0.981 | 7.303 | 7.846 | 0.463 | 1.50 7 | 0.494 | 1.365 | 4.47 5 |
| 7.857 | 14.3 | 0.381 7 | 0.959 5 | 0.5778 | 2.86 | 0.878 | 7.017 | 6.598 | 0.378 | 1.44 2 | 0.442 | 1.307 | 4.00 6 |

Table.3(b): Impact of various ratios of FA for the 297.15K redox region..

| [M] x10 ⁻³ | [L] x10 ⁻⁴ | Ep,a | Ep,c | ΔEp | (-)Ip,a x10 ⁻⁵ | Ip,c x10 ⁻⁴ | Da x10 ⁻¹⁴ | Dc x10 ⁻¹² | Ks | Γ a x10 ⁻⁹ | Γ c x10 ⁻⁸ | (-) Q a x10 ⁻⁵ | (+) Qc x10 ⁻⁴ |
|-----------------------|-----------------------|------------|------------|------------|---------------------------|------------------------|-----------------------|-----------------------|------------|-----------------------|-----------------------|---------------------------|--------------------------|
| 8.93 | 2.71 | 0.25 42 | 0.97 35 | 0.71 93 | 9.858 | 4.968 | 64.51 | 16.38 | 17.1 51 | 4.57 4 | 2.305 | 5.048 | 2.544 |
| 8.68 | 5.26 | 0.25 60 | 0.97 11 | 0.71 51 | 9.013 | 4.579 | 56.87 | 14.68 | 14.9 24 | 4.18 1 | 2.124 | 4.615 | 2.345 |
| 8.35 | 8.86 | 0.26 56 | 0.95 81 | 0.69 25 | 5.281 | 3.762 | 21.09 | 10.71 | 8.89 0 | 2.45 0 | 1.745 | 2.704 | 1.927 |
| 8.25 | 10.0 | 0.29 27 | 0.95 71 | 0.66 44 | 2.570 | 3.241 | 5.123 | 8.147 | 4.70 9 | 1.19 2 | 1.504 | 1.316 | 1.660 |
| 8.05 | 12.2 | 0.38 63 | 0.93 36 | 0.54 73 | 1.311 | 2.474 | 1.400 | 4.987 | 0.42 2 | 0.60 8 | 1.148 | 0.671 | 1.267 |
| 7.86 | 14.3 | 0.38 63 | 0.92 91 | 0.54 28 | 1.195 | 1.875 | 1.221 | 3.007 | 0.35 0 | 0.55 4 | 0.870 | 0.611 | 0.960 |

Impact of various scan speeds

The relationship among NCS and FA was examined in relation to the impact of various scan speeds (0, 1, 0.05, 0.02, and 0.01)(V/sec), as shown in Fig. 7. Then, Table.4 can be used to calculate the solvation and kinetic values at the various scan rates (a,b). It was found that the maxima decreased by decreasing in the scan rate and also decreased in all parameters at 297.15K than that of 292.15K due the complexation character. In 0.1M KBr, Fig. 8 also depicted the relationship among both cathodic and anodic peak current I_p and the square root of scan rate.

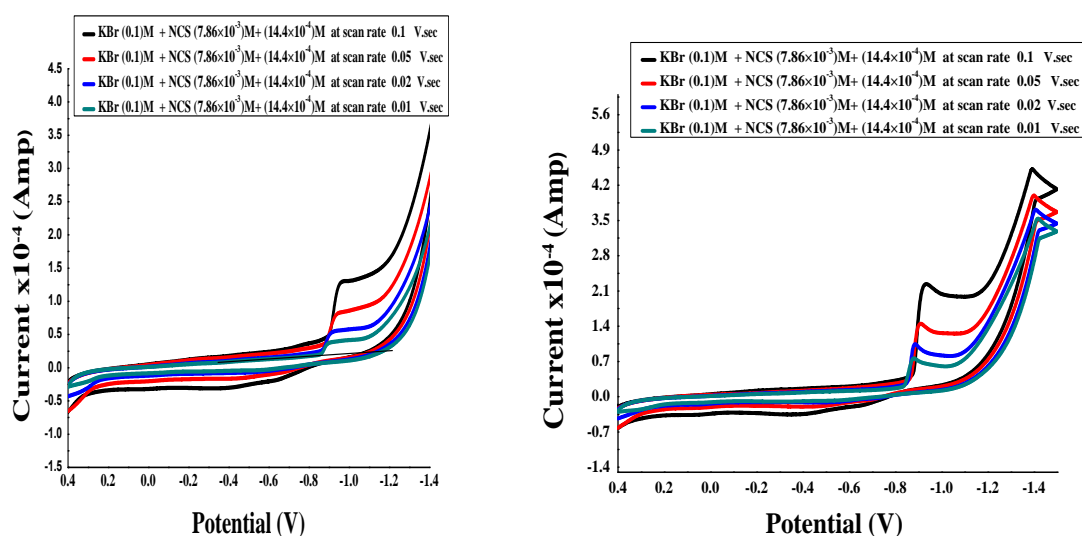


Fig.(7): Impact of various scan speeds of (7.86×10^{-3}) M FA with (14.3×10^{-4}) M NCS at (a) 292.15 K (b) 297.15 K.

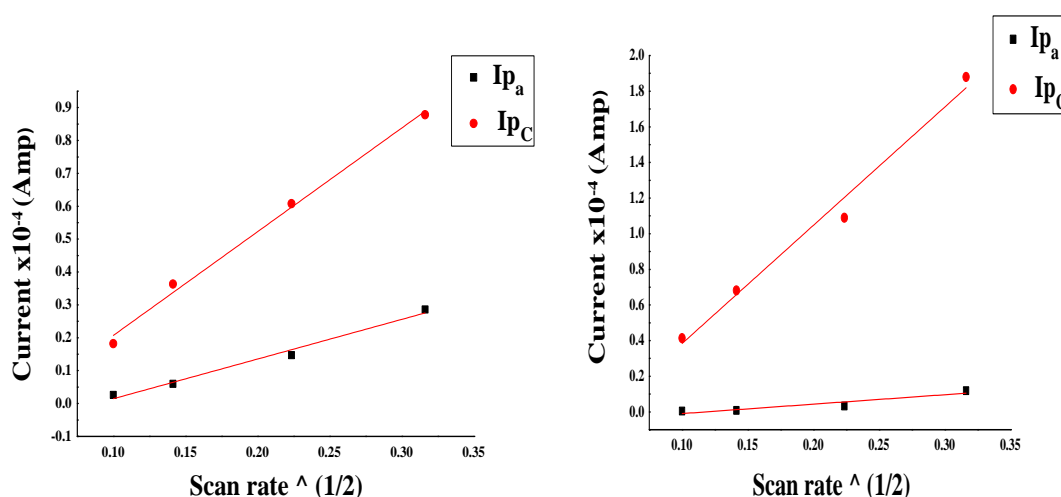


Fig.(8):The relation between peak current I_p (I_{p_c} – I_{p_a}) among the square root of various scan speeds in the existence of FA at (a) 292.15K (b) 297.15K.

Table.4(a): Effects of various complex scan rates for the 292.15K redox region.

| v | E _{pa} | E _{pc} | ΔE _p | (-)I _{pa} x10 ⁻⁵ | I _{pc} x10 ⁻⁵ | D _a x10 ⁻¹⁵ | D _c x10 ⁻¹³ | k _s | Γ _a x10 ⁻⁹ | Γ _c x10 ⁻⁹ | (-)Q _a x10 ⁻⁵ | (+)Q _c x10 ⁻⁵ |
|------|-----------------|-----------------|-----------------|---|--------------------------------------|--------------------------------------|--------------------------------------|----------------|-------------------------------------|-------------------------------------|--|--|
| 0.1 | 0.3917 | 0.9695 | 0.5878 | 2.874 | 8.718 | 7.027 | 6.588 | 0.3786 | 1.317 | 4.106 | 1.452 | 4.4221 |
| 0.05 | 0.4318 | 0.9586 | 0.5669 | 1.479 | 6.018 | 3.694 | 6.320 | 0.0868 | 1.350 | 5.650 | 1.490 | 6.1261 |
| 0.02 | 0.4742 | 0.9325 | 0.4483 | 0.597 | 3.613 | 1.540 | 5.649 | 0.0153 | 1.374 | 8.284 | 1.516 | 9.1421 |
| 0.01 | 0.4842 | 0.9103 | 0.4361 | 0.258 | 1.811 | 0.575 | 2.835 | 0.0060 | 1.183 | 8.293 | 1.285 | 9.1511 |

Table.4(b): Effects of various complex scan rates for the 297.15K redox region.

| v | E _{pa} | E _{pc} | ΔE _p | (-)I _{pa} x10 ⁻⁵ | I _{pc} x10 ⁻⁴ | D _a x10 ⁻¹⁶ | D _c x10 ⁻¹² | k _s | Γ _a x10 ⁻¹⁰ | Γ _c x10 ⁻⁸ | (-)Q _a x10 ⁻⁶ | (+)Q _c x10 ⁻⁴ |
|------|-----------------|-----------------|-----------------|---|--------------------------------------|--------------------------------------|--------------------------------------|----------------|--------------------------------------|-------------------------------------|--|--|
| 0.1 | 0.3863 | 0.9291 | 0.5428 | 1.195 | 1.875 | 122.1 | 3.007 | 0.350 | 5.543 | 0.8700 | 6.119 | 0.9603 |
| 0.05 | 0.4738 | 0.9067 | 0.4329 | 0.331 | 1.094 | 18.80 | 2.046 | 0.028 | 3.076 | 1.015 | 3.395 | 1.120 |
| 0.02 | 0.5040 | 0.8838 | 0.3798 | 0.0809 | 0.682 | 2.805 | 1.992 | 0.008 | 1.879 | 1.583 | 2.074 | 1.747 |
| 0.01 | 0.5039 | 0.8756 | 0.3717 | 0.0400 | 0.414 | 1.368 | 1.469 | 0.004 | 1.856 | 1.923 | 2.048 | 2.123 |

Nature of the complexation involving NCS and FA electrochemically.

Through using given equations [43–48], the stability constants (β_{MX}) for CoSO₄ complexes at each addition are computed:

$$\Delta E^\circ = (E^\circ_{\text{C}} - E^\circ_{\text{M}}) = 2.303 (RT/nF) * (\log \beta_{\text{MX}} + j \log C_x) \quad (7)$$

$$E^\circ = (E_{\text{pa}} + E_{\text{pc}})/2 \quad (8)$$

$$\Delta G = (-2.303 RT \log \beta_{\text{MX}}) \quad (9)$$

Where; R was a gas constant (8.314 J.mol⁻¹.degree⁻¹), T was the absolute temperature, j was the coordination number of the stoichiometric complex, and C_x was the amount of FA in the solution. Where E[°]_M was the formal peak potential of metal EC was the formal peak potential of the metal complex following each addition of FA, and at last adding in the missing of FA. E_{pa} and E_{pc} were the anodic and cathodic peak potentials, respectively, and the stability constant (β_{MX}).was used to calculate the Gibbs free energy of contact (G) for NCS with FA.

Fig. 9 depicts the relationship between the Gibbs free energy and stability constant of CoSO₄ complexes with FA.

The enthalpy (H) of contact for NCS with FA was estimated utilizing Van't Hoff formula (10).

$$\log \frac{\beta_{\text{MX at } (T_2)}}{\beta_{\text{MX at } (T_1)}} = \frac{\Delta H}{2.303} \left(\frac{T_2 T_1}{T_2 - T_1} \right) \quad (10)$$

where T₂ and T₁ are both 292.15 K and 297.15 K, respectively, and β_{MX} was the stability constant at various temperatures.

Additionally, using Eq., the entropy (S) for the synthesized complex among NCS and FA at the two various temperatures was being estimated (11)

$$\left(\Delta S = \frac{\Delta H - \Delta G}{T} \right) \quad (11)$$

The obtained values of β_{MX}, ΔG, ΔH, and ΔS of the synthesized complex were shown in **Table.5**.

It was observed positive entropy values, negative free energies indicating spontaneous reactions and positive enthalpies due to reactions are endothermic. By raising FA, the Gibbs free energies increased, indicates a greater contact.

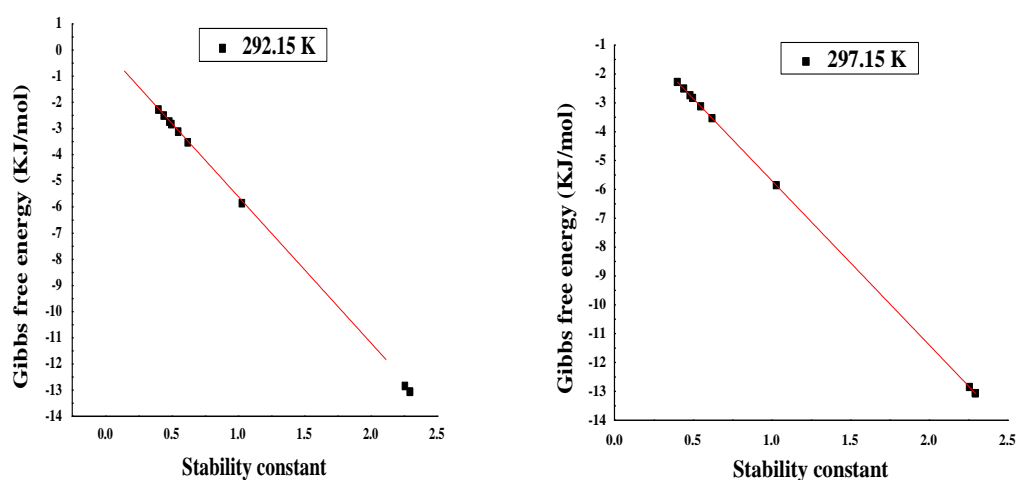


Fig.(9): The relationship among both Gibbs free energy and Stability constant values for the prepared Complex at (a) 292.15K (b) 297.15K.

Table.5: stability constant β_{MX} , enthalpy ΔH , Gibbs free energy ΔG and The entropy of connection ΔS for the synthesized complexes at 292.15 and 297.15K.

| Conc of [M] $\times 10^{-3}$ | Conc of [L] $\times 10^{-4}$ | j | log β_j | | Gibbs free energy | | ΔH (KJ/mol) | entropy |
|------------------------------|------------------------------|--------|---------------|--------|-------------------|----------|---------------------|---------|
| | | | 292.15K | 297.15 | 292.15K | 297.15 | | |
| 9.041 | 1.370 | 0.0152 | 0.2310 | 0.4979 | -1.2921 | -2.8327 | 716.58 | 2.457 |
| 8.919 | 2.703 | 0.0303 | 0.1429 | 0.4001 | -0.7994 | -2.2763 | 930.64 | 3.188 |
| 8.800 | 4.000 | 0.0455 | 0.3776 | 0.4407 | -2.1120 | -2.5076 | 388.07 | 1.336 |
| 8.684 | 5.263 | 0.0606 | 0.5187 | 0.4813 | -2.9017 | -2.7385 | 296.07 | 1.023 |
| 8.571 | 6.494 | 0.0758 | 0.9448 | 0.6206 | -5.2849 | -3.5312 | 218.39 | 0.766 |
| 8.354 | 8.861 | 0.1061 | 1.3928 | 0.5484 | -7.7909 | -3.1200 | 130.89 | 0.475 |
| 8.250 | 10.00 | 0.1212 | 1.6407 | 1.0297 | -9.1779 | -5.8586 | 208.64 | 0.746 |
| 8.148 | 11.11 | 0.1364 | 1.7029 | 2.2960 | -9.5258 | -13.0631 | 448.22 | 1.567 |
| 8.049 | 12.20 | 0.1515 | 1.8177 | 2.2964 | -10.1677 | -13.0653 | 419.99 | 1.472 |
| 7.952 | 13.25 | 0.1667 | 1.9089 | 2.2582 | -10.6778 | -12.8482 | 393.28 | 1.383 |
| 7.857 | 14.29 | 0.1818 | 2.1147 | 2.2959 | -11.8291 | -13.0626 | 360.93 | 1.276 |

V –CONCLUION

The redox behavior of nano cobalt salt (NCS) in absence and existence of the fuchsin acid (FA) was studied at both various temperatures by new stuffed nano composite glassy carbon electrode. The solvation cyclic voltammetry data was obtained and their values were compared. The different thermodynamic parameter, stability constant, Gibbs free energies of solvation, entropies and enthalpies of solvation indicate the complexation of cobalt ions and fuchsin acid (FA). At last, through using Molecular Operating Environment (MOE) and human Myosin 9b RhoGAP domain crystalline phase at 2.2 Angstrom, a molecular modelling study was conducted to explain the studied anticancer activity of FA (5C5S).

Conflict of Interest

There are no Conflict of Interest in this study, and it has received no outside funding.

REFERENCES

1. R. Wever, K. Kustin, *Adv. Inorg. chem.*, 35 (1990) 81–115.
2. D. Rehder, *Angew. Chem.*, 103 (1991)152–172.
3. A. Butler, C.J. Carrano, *Coord. Chem. Rev.*, 109 (1991) 61–105.
4. E. Hoppe, C. Limberg, *Chem. Eur.*, 13 (2007) 7006.
5. M. Xie, L. Gao, L. Li, W. Liu, S. Yan, *J. Inorg. Biochem.*, 99 (2005) 546–551.
6. A. Sheela, R. Vijayaraghavan, *J. Coord. Chem.* 64 (2011) 511.
7. Y. Wei, C. Chan, J. Tian, G. Jang, K.F. Hsueh, Terthiophene : *Chem. Mater.*, (1991) 888–897.
8. S.N. Haier, S. Park, *J. Electrochem. Soc.*, 140 (1993) 2454–2463.
9. J.E.B. Randles, *Trans. Faraday. Soc.* 44 (1948) 327–338.
10. S.H. Sun, *Adv. Mater.*, 18(2006)393.
11. C.B. Murray, C.R. Kagan, M.G. Bawendi, *Science*, 270 (1995)1335.
12. A.P. Alivisatos, *Science*, 27 (1996) 933.
13. A.H. Lu, E.L. Salabas, F. Schuth, *Angew. Chem. Int. Ed.*, 46 (2007) 1222.
14. D.P. Dinepa, M.G. Bawendi, *Angew. Chem. Int. Ed.*, 38 (1999) 1788.
15. Q.A. Pankhurst, J. Connolly, S.K. Jones, J. Dobson, *J. Phy. D. Appl. Phys.*, 36 (2003).
16. J. Wang, J.D. MacNEIL, J.F. Kay, John Wiley. (2012) 464.
17. W.L. Holman, *J. Infect. Dis.*, 15 (1914) 227–233.
18. Morsi, A. Mohamed, E.A. Gomaa, and A.S. Nageeb. *Asian J. Nanosci. Mat.*, 1,4 (2018) 282-293.
19. S.E. Salem, E.A. Gomaa, M.M. El-Defrawy, N.M. Ebrahim, *European J. Adv. Chem. Res.*, 2,1 (2021) 14-20.
20. M. Fathi, S.E. Salem, E.A. Gomaa, H.M. Killa. *Egypt. J. Chem.*, 63,12 (2020) 5239-5249.
21. E. Muller, *Electrochem.*, 13, 133 (1907).
22. S.T. Mayer, R.H. Muller, *J. Electrochem. Soc.*, 139, 426 (1992).
23. M.N. Abd EL-Hady, Esam A. Gomaa, Anwer G. Al-Harazie, *J. Mol. Liq.*, 276 (2019) 970-985.
24. M.N. Abd El-Hady, E. A. Gomaa, R.R. Zaky, A.I. Gomaa, *J. Mol. Liq.*, 305 (2000) 112794.
25. E.A. Gomaa, S. E. Salem, *American Assoc. Sci. Technol. Commun.*, 3 (2016) 160-168.
26. M.M. El-Defrawy, E.A. Gomaa, S. E. Salem, F.M. Abdel Razek, *Prog. Chem. Biochem. Res.*, 1 (2018) 11-18.
27. S. E. Salem, E A. Gomaa, M M. El-Defrawy, N. M. Mohamed, *European J. Adv. Chem. Res.*, 2 (2021).
28. E.M. Abou Elleel, E.A. Gomaa, M.S. Mashally, *J. Biochem. Tech.*, 9 (2) (2018) 42-47.
29. E.A. Gomaa, M.A. Berghot, Mohamed R. Moustafa, Fathy M. Eltaweel, Hadeer M. Farid, *J. Mart. Environ. Sci.*, 10 (2019) 187-194.
30. L.I. Ali, S.A. Abdel Halim, E.A. Gomaa, S.G. Sanad, *Iran. J. Chem. Eng.*, 38 (2019) 43-58.
31. E.A. Gomaa, R.R. Zaki, M.S. Nouh, *Adv. J. Chem. Section A.*, 3 (2020) 1-18.
32. F.A. Cotton, G. Wilkinson, *Adv. Inorg. Chem.*, 4th Ed., John Willey & Sons, New York, (1980).

33. P.L. Timmanagoounder, G.A.A. Hiremath, S.T. Nandibewoor, *Trans. Met. Chem.*, 22 (1997)193-196.
34. Y. Wang, R.M. Hernandez, D.J. Bartlett, J.M. Bingham, T.R. Kline, A. Sen & T.E. Mallouk, *Langmuir*, 22 (2006) 10451-10456.
35. A.E. El-Askalany & A.M. Abou El-Magd, *Chem. Pharm. Bull.*, 43 (1995) 1791-1792.
36. E.A. Gomaa, R.M. Abu-Qarn, *J. Mol. Liq.*, 232 (2017) 319-324.
37. E.A. Gomaa, M.A. Tahoona, A. Negm, *J. Mol. Liq.*, 241(2017) 595-602.
38. E.A. Gomaa, R.R. Zaky, A. Shokr, *J. Mol. Liq.*, 232 (2017) 319-324.
39. E.A. Gomaa, R.R. Zaky, A. Shokr, *Chem. Data Collect.*, 11(2017) 67-76.
40. E.A. Gomaa, A. Negm, M.A. Tahoona, *J. Taibah Univ. Sci.*, 11 (2017) 741-748.
41. S.E. El-Shereafy, E.A. Gomaa, A.M. Yousif, A.S. El-Yazed, *Iran. J. Mat. Sci. Eng.*, 14 (2017) 48-57.
42. D.A.C. Brownson, C.E. Banks, *The Handbook of Graphene Electrochemistry.*, Springer, (2014).
43. E.A. Gomaa, M.A. Tahoona, *M.A J. Mol. Liq.*, 214 (2016) 19-23.
44. J. Wang, *Anal. Electrochem.*, 3rd ed., Jhon Wiley & Sons., Inc.; London, (2006).
45. E.A. Gomaa, M.A. Tahoona, A. Shokr; *Chem. Data Collect.*, 3, (2016) 58-67.
46. E.A. Gomaa, M.H. Mahmoud, M.G. Mousa, E.M. El-Dahshan, *Chem. Method.*, 3 (2018) 1-11.
47. E.A. Gomaa, G. Begheit, *Asian J. Chem.*, 2 (1990) 444.
48. E.A. Gomaa, Radwa T. Rashed, *Biom. J. Sci. Tech. Res.*, 23 (2019) 17345-17349.